The coding microsatellite mutation profile of PMS2-deficient colorectal cancer

Bajwa-ten Broeke, S.W.; Ballhausen, A.; Ahadova, A.; Suerink, M.; Bohaumilitzky, L.; Seidler, F.; ... ; Kloor, M.

Experimental and Molecular Pathology 122 (2021) 104668

Contents lists available at ScienceDirect

Experimental and Molecular Pathology

journal homepage: www.elsevier.com/locate/yexmp

The coding microsatellite mutation profile of PMS2-deficient colorectal cancer

Sanne W. Bajwa - ten Broeke [a,b,*,1], Alexej Ballhausen [c,f,g,1], Aysel Ahadova [c,g], Manon Suerink [b], Lena Bohaumilitzky [c,g], Florian Seidler [c,g], Hans Morreau [d], Tom van Wezel [d], Julia Krzykalla [e], Axel Benner [e], Noel F. de Miranda [d], Magnus von Knebel Doeberitz [c,g], Maartje Nielsen [b,2], Matthias Kloor [c,g,2]

[a] Department of Genetics, University Medical Center Groningen, Groningen, the Netherlands
[b] Department of Clinical Genetics, Leiden University Medical Center, Leiden, the Netherlands
[c] Department of Applied Tumor Biology, Institute of Pathology, University Hospital Heidelberg, Cooperation Unit Applied Tumor Biology, German Cancer Research Center (DKFZ), Heidelberg, Germany
[d] Department of Pathology, Leiden University Medical Center, Leiden, the Netherlands
[e] Division of Biostatistics, German Cancer Research Center (DKFZ), Heidelberg, Germany
[f] Department of Hematology, Oncology and Tumor Immunology, Charité–Universitätsmedizin Berlin, Berlin, Germany
[g] Molecular Medicine Partnership Unit (MMPU), University Hospital Heidelberg, Heidelberg, Germany

ARTICLE INFO

Keywords:
HNPCC
Molecular pathways
Hereditary colorectal cancer
Immunology of cancer

ABSTRACT

Lynch syndrome (LS) is caused by a pathogenic heterozygous germline variant in one of the DNA mismatch repair (MMR) genes: *MLH1*, *MSH2*, *MSH6* or *PMS2*. LS-associated colorectal carcinomas (CRCs) are characterized by MMR deficiency and by accumulation of multiple insertions/deletions at coding microsatellites (cMS). MMR deficiency-induced variants at defined cMS loci have a driver function and promote tumorigenesis. Notably, *PMS2* variant carriers face only a slightly increased risk of developing CRC. Here, we investigate whether this lower penetrance is also reflected by differences in molecular features and cMS variant patterns. Tumor DNA was extracted from formalin-fixed paraffin-embedded (FFPE) tissue cores or sections (n = 90). Tumors originated from genetically proven germline pathogenic MMR variant carriers (including 14 PMS2-deficient tumors). The mutational spectrum was analyzed using fluorescently labeled primers specific for 18 cMS previously described as mutational targets in MMR-deficient tumors. Immune cell infiltration was analyzed by immunohistochemical detection of T-cells on FFPE tissue sections. The cMS spectrum of PMS2-deficient CRCs did not show any significant differences from MLH1/MSH2-deficient CRCs. PMS2-deficient tumors, however, displayed lower CD3-positive T-cell infiltration compared to other MMR-deficient cancers (28.00 vs. 55.00 per 0.1 mm^2, p = 0.0025). Our study demonstrates that the spectrum of potentially immunogenic cMS variants in CRCs from *PMS2* gene variant carriers is similar to that observed in CRCs from other MMR gene variant carriers. Lower immune cell infiltration observed in PMS2-deficient CRCs could be the result of alternative mechanisms of immune evasion or immune cell exclusion, similar to those seen in MMR-proficient tumors.

1. Introduction

Lynch syndrome (OMIM 120435) is caused by a pathogenic heterozygous germline variant in one of the DNA mismatch repair (MMR) genes *MLH1* (OMIM 120436), *MSH2* (OMIM 609309), *MSH6* (OMIM 600678) or *PMS2* (OMIM 600259). After somatic inactivation of the remaining functional MMR gene allele, MMR deficiency leads to the accumulation of numerous small insertions or deletions at repetitive sequence stretches termed microsatellites (microsatellite instability, MSI). Insertions or deletions affecting microsatellites located in gene-

* Corresponding author at: Antonius Deusinglaan 1, 9713 AV Groningen, the Netherlands.
E-mail address: s.w.ten.broeke@umcg.nl (S.W. Bajwa - ten Broeke).
[1] Bajwa - ten Broeke and Ballhausen contributed equally as first authors.
[2] Nielsen and Kloor contributed equally as last authors.

https://doi.org/10.1016/j.yexmp.2021.104668
Received 9 June 2021; Accepted 19 July 2021
Available online 22 July 2021

encoding regions can lead to shifts of the translational reading frame and thus to inactivation of the affected genes. Moreover, through shifting of the reading frame, completely new peptide sequences are synthesized that are unknown to the immune system and therefore can elicit strong immune responses of the host (Schwitalle et al., 2008; Le et al., 2017). Several coding microsatellite (cMS) variants that drive Lynch syndrome cancer progression through the inactivation of tumor suppressor genes have been previously identified (Alhopuro et al., 2012; Woerner et al., 2003). As cMS variants can contribute to cancer development, the patterns of cMS variants observed in manifest cancers reflect evolutionary selection and therefore the pathogenesis of tumor developments. This is exemplarily illustrated by marked differences in cMS variant frequency between colorectal and endometrial carcinomas (Kim et al., 2013; Hause et al., 2016).

Carriers of a pathogenic variant in the *PMS2* gene have a markedly lower penetrance and later age of onset of colorectal and endometrial cancer than carriers of pathogenic *MLH1* or *MSH2* variants (ten Broeke et al., 2015; Senter et al., 2008; Ten Broeke et al., 2018a). The reported cumulative risk of CRC is 11–20% for *PMS2* carriers, which is in sharp contrast to a cumulative risk of 35–55% up to age 70 for *MLH1/MSH2* carriers (Barrow et al., 2013). Notably, prospective studies have now reported that the cumulative risk of colorectal cancer for *PMS2* variant carriers undergoing colonoscopic surveillance and polypectomies is 0% (Ten Broeke et al., 2018a). This is in contrast to *MLH1/MSH2* carriers with risks of CRCs arising between follow-up colonoscopies to be up to 46% and 43% respectively. Even *MSH6* carriers who also have a milder phenotype are at risk (15%) of such incident cancers (Moller et al., 2017). Consequently, the functional significance of pathogenic *PMS2* variants during the pathogenesis of cancers has been questioned and it is perceivable that *PMS2* deficiency may play a different and potentially less prominent role in tumorigenesis.

A previous study by Alpert and colleagues reported that CRCs with isolated PMS2 loss (i.e. without concomitant MLH1 loss) displayed less histological features associated with MSI (i.e. tumor-infiltrating lymphocytes (TILs), Crohn's-like lymphocytic reaction, mucinous or signet ring cell component and medullary growth pattern) (Alpert et al., 2018). Their data also suggested that these tumors might display a more aggressive behavior, with an odds ratio of 3.87 (95% CI: 0.89–27.04) for disease-specific death when the analyses were restricted to germline variant or probable Lynch syndrome cases only. They hypothesized that these observations might be related to a lower degree of immune activation potentially resulting from a smaller number of immunogenic frameshift peptide neoantigens produced in PMS2-deficient tumors.

We have recently developed a novel tool to quantify immunogenic cMS mutations in MSI cancer (Ballhausen et al., 2020). In the present study, we used this approach to compare cMS variant patterns in PMS2-deficient CRCs from confirmed carriers to those observed in CRCs from *MLH1* and *MSH2* variant carriers.

2. Material and methods

2.1. Tumor specimens

Tumor material from 10 confirmed pathogenic germline *PMS2* variant carriers was collected at Leiden University Medical Centre. Tumor material from 41 *MLH1*, 21 *MSH2*, and 4 *PMS2* carriers was collected at the Department of Applied Tumor Biology, Institute of Pathology, University Hospital Heidelberg, as a center of the German Consortium for Familial Intestinal Cancer. Informed consent was obtained from all participating patients. The study was approved by the Institutional Ethics Committee (Protocol number: S-583/2016). Additional data on age at diagnosis, tumor histology and tumor stage was extracted from pathology reports when available.

2.2. Tumor workup and DNA isolation

Tissue blocks were collected, and DNA was isolated from three tissue cores of variable length (0.3 mm diameter, or 0.7 mm in case of tissue with a low cell count) or from whole tissue sections after manual microdissection using the DNeasy FFPE Kit (Qiagen, Germany).

2.3. Microsatellite analysis

For the characterization of cMS patterns, we performed fragment length analysis using fluorescently labeled primers specific for a selected series of 18 coding microsatellites previously described as mutational targets in MSI cancer development. (Woerner et al., 2010) Selection criteria were (Schwitalle et al., 2008) frequency of variant in MMR-deficient cancers, (Le et al., 2017) evidence of a functional driver role of variants suggested by a pathogenic variant frequency higher than expected from microsatellite length, and (Alhopuro et al., 2012) potential significance as source of immunogenic frameshift peptide neoantigens supported by MHC binding prediction algorithms. PCR products were visualized on an ABI3130*xl* sequencer, and the obtained results were processed using a newly developed algorithm to obtain quantitative estimation of the frequency of the mutant alleles in tumor specimens (ReFrame) (Ballhausen et al., 2020). CMS analyses demonstrated in this study are partially based on our previous report with a re-analysis of mutation data with regard to differences between MMR variant carriers.

2.4. Immunohistochemical analysis of CD3

From 11 PMS2-, 13 MLH1- and 14 MSH2-deficient tumors formalin fixed paraffin embedded (FFPE) tumor blocks were available for further analysis of immune cell infiltration. For immunohistochemical detection of CD3-positive cells, 4 μm thick sections of the tumors were stained with an antibody specific for CD3 (1:60 dilution, Acris, Cat. No.: DM112, clone PS1). In short, sections were deparaffinized and endogenous peroxidase was inactivated with H_2O_2 in methanol solution (0.3%). After this, heat-induced antigen retrieval was performed in a 10 mM citrate buffer (pH 6). Sections were incubated with the anti-CD3 antibody overnight at 4° followed by incubation with poly-HRP and staining with 3,3′-Diaminobenzidine. Slides were counterstained with hematoxylin. For immune cell scoring 4 areas of interest (0.1 mm^2 each) were randomly placed in the tumor center, CD3-positive immune cell infiltration was scored as the mean number of CD3-positive immune cells of the 4 areas (Fig. 1).

2.5. Statistical analysis

Gene-wise variant rates were compared in three steps: First, all cMS showing a prevalence of at least 15% non-wild type alleles in a certain tumor were classified as mutant. The pathogenic variant status was compared between tumors from PMS2 carriers and those from MLH1 and MSH2 carriers grou- ped together using fisher's exact test. Holm method was used to adjust the raw *p*-values over all genes. Adjusted *P* values smaller than 0.05 were defined as statistically significant.

In a second step, quantitatively analyzed mutant allele ratios were used to test for differences in cMS variant patterns between tumors from PMS2 carriers and those from MLH1 and MSH2 carriers grouped together. For this, Wilcoxon-Mann-Whitney test was used and raw *p*-values were adjusted over all genes using Holm method. Finally, quantitatively analyzed cMS patterns of PMS2-deficient CRCs were separately tested against those with MLH1- or MSH2-deficiency. The global p-value states if there is a significant difference for at least one of the two pairwise comparisons (PMS2 vs. MLH1 or PMS2 vs. MSH2) in the relative effects. The pairwise *p*-values give the results for local pairwise comparison. Then, a two-sample Kolmogorov-Smirnov test was applied for the pairwise comparisons in order to test for equal distribution.

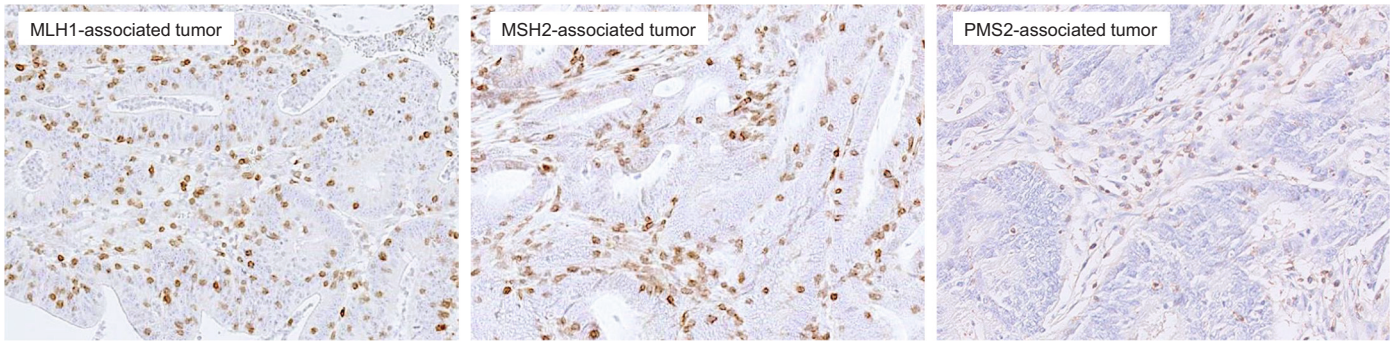

Fig. 1. Examples of slides used for immune cell scoring. CD3-positive immune cell infiltration was scored as the mean number of CD3-positive immune cells of the 4 areas of interest (0.1 mm^2 each), randomly placed in the tumor center.

Pairwise p-values for both approaches were adjusted over all genes using Holm method.

Additionally, T-cell infiltration measured by mean number of CD3-positive T cells was compared between *PMS2* and *MLH1/MSH2* groups. Wilcoxon-Mann-Whitney test was applied in order to test the difference in median CD3-positive T-cell infiltration between two groups. Results were also compared with a sporadic MSI CRC cohort ($n = 47$).

3. Results

3.1. Clinical characteristics

A description of clinical characteristics of the analyzed cohorts is available in Table 1. Of note, PMS2-deficient CRCs displayed a higher tumor stage compared to the MLH1/MSH2 cohorts ($p = 0.0351$).

3.2. Comparison of cMS variant frequency between PMS2- and non-PMS2-deficient CRCs

Tumors from 14 *PMS2*, 35 *MLH1* and 20 *MSH2* carriers were analyzed for cMS variant patterns (Table 2). Interpretable results were obtained for a median number of 58 tumors per cMS gene and ranged from 51 to 65 tumors per gene. Five out of 18 analyzed cMS showed variants in all analyzable PMS2-deficient CRCs: *ACVR2* ($n = 12$), *AIM2* (n = 12), *BANP* (n = 12), *C4orf6* ($n = 10$), *ZNF294* (n = 12). Common functionally relevant target cMS presented with similar variant frequencies in PMS2 vs. non-PMS2-deficient CRCs, including *ACVR2* (PMS2: 12/12, 100% vs non-PMS2: 46/51, 90.2%, $p = 1.00$), *AIM2* (PMS2: 12/12, 100% vs. non-PMS2: 42/48, 87.5%, $p = 0.69$), and *TGFBR2*, the most commonly analyzed cMS target in MMR-deficient colorectal cancer (PMS2: 9/11, 81.8% vs. non-PMS2: 41/44, 93.2%, p = 1.00).

No significant differences in cMS variant frequencies were observed between CRCs from *PMS2* carriers and CRCs from *MLH1* and *MSH2* carriers after adjusting for multiple testing (Table 2).

In order to evaluate whether PMS2-deficient tumors may show a quantitative difference in cMS variants compared to MLH1- and MSH2-deficient CRCs, we quantitatively analyzed cMS variant profiles (Table 3). After adjusting for multiple testing, there were no significant differences between cMS mutated allele ratios of PMS2- and MLH1-/MSH2-deficient CRCs. Of borderline significance, 10 PMS2-deficient CRCs had a higher cMS mutant allele ratio in *C4orf6* than 47 MLH1- and MSH2-deficient CRCs (0.434 vs. 0.253, $p = 0.07$).

Table 1
Description of the cohort.

	PMS2 ($n = 14$)	MLH1 ($n = 41$)	MSH2 ($n = 21$)
Gender			
Male	7 (50%)	19 (46%)	11 (52%)
Female	7 (50%)	19 (46%)	9 (43%)
Unknown	0	3 (7%)	1 (5%)
Age at CRC diagnosis			
Median (IQR)	48.0 (46.0–56.5)	48.0 (41.2–62.3)	47.0 (42.5–53.9)
Mean (SD)	51.3 (13.3)	51.3 (13.4)	49.2 (9.5)
Unknown	2	8	5
Tumor stage (UICC)			
1	1 (7%)	13 (32%)	2 (10%)
2	7 (50%)	11 (27%)	10 (48%)
3	4 (27%)	6 (15%)	1 (5%)
4	1 (7%)	0 (0%)	1 (5%)
Unknown	1 (7%)	11 (27%)	7 (33%)
Location			
Proximal	9 (64%)	21 (51%)	7 (33%)
Distal	4 (29%)	11 (27%)	6 (29%)
Unknown	1 (7%)	9 (22%)	8 (38%)
MSI			
Stable	1 (7%)	0	0
High	12 (85%)	41 (100%)	21 (100%)
Unknown	1 (7%)	0	0
***B2M* status**			
Wildtype	11 (79%)	23 (56%)	11 (52%)
Mutated	1 (7%)	11 (26.8%)	4 (19%)
Unknown	2 (14%)	7 (17%)	6 (28%)

3.3. Quantitative analysis of intratumoral CD3-positive lymphocyte infiltration

As a next step, we analyzed the density of tumor-infiltrating lymphocytes in tumors from *PMS2* ($n = 11$), *MLH1* ($n = 13$), and *MSH2* ($n = 14$) carriers. The analysis of CD3-positive lymphocyte infiltration revealed significantly lower median CD3-positive T-cell counts per 0.1 mm^2 in PMS2-deficient CRCs when compared to MLH1- and MSH2-deficient CRCs (28.00 vs. 55.00, $p = 0.0025$, Fig. 2).

In order to account for a potential overrepresentation of high stage tumors in the PMS2 cohort, we performed a stratified analysis on UICC tumor stage. The difference in CD3-positive T-cell count remained statistically significant for the comparison of UICC III + IV for the PMS2 vs. the non-PMS2 cohort (19.50 vs. 82.37, $p = 0.0286$, Fig. 3).

3.4. Analysis of B2M mutation status

To assess, whether the observed difference of lower CD3-positive T-cell counts in PMS2 associated cancers correlated with a difference in mutation frequency of *B2M*, the mutation frequency of *B2M* was analyzed by sanger sequencing. Of interest, the *B2M* mutation frequency of 10 *PMS2* associated cancers (10%, 1/10 *B2M* mutation frequency) and 32 *MLH1*- or *MSH2* associated cancers (43.8%, 14/32 *B2M* mutation frequency) did not differ significantly ($p = 0.2556$, Table 1), although a trend towards fewer mutations in *B2M* was observed in the *PMS2* associated cohort. As a next step, the influence of tumor stage on *B2M* mutation frequency was analyzed. Interestingly, the *B2M* mutation frequency of 4 *PMS2* associated high stage (UICC III and IV) cancers

Table 2
Percentage of tumors harboring variants.

cMS	Variant frequency (PMS2)	Sample number (PMS2)	Variant frequency (MLH1 + MSH2)	Sample number (MLH1 + MSH2)	p value	Adjusted p value
ACVR2A	100,0%	12	90,2%	51	1.00	1.00
AIM2	100,0%	12	87,5%	48	0.57	1.00
ASTE1	75,0%	12	89,4%	47	0.33	1.00
BANP	100,0%	12	95,3%	43	1.00	1.00
C4orf6	100,0%	10	59,6%	47	**0.02**	0.40
CASP5	54,5%	11	75,0%	44	0.26	1.00
ELAVL3	50,0%	10	64,4%	45	1.00	1.00
GLYR1	54,5%	11	58,0%	50	0.73	1.00
LMAN1	45,5%	11	54,0%	50	0.50	1.00
MARCKS	90,9%	11	88,1%	42	1.00	1.00
NDUFC2	76,9%	13	88,6%	44	0.37	1.00
PTHLH	66,7%	12	68,0%	50	0.47	1.00
SLC22A9	91,7%	12	86,4%	44	1.00	1.00
SLC35F5	91,7%	12	55,3%	47	**0.04**	0.68
TAF1B	90,9%	11	82,4%	51	0.67	1.00
TCF7L2	75,0%	8	69,8%	43	1.00	1.00
TGFBR2	81,8%	11	93,2%	44	0.57	1.00
ZNF294	100,0%	12	94,3%	53	1.00	1.00

Table 3
Frequency of mutant alleles.

cMS	Mutant allele ratio (PMS2)	Sample number (PMS2)	Mutant allele ratio (MLH1 + MSH2)	Sample number (MLH1 + MSH2)	p value	Adjusted p value
ACVR2A	0.503	12	0.506	51	0.62	1.00
AIM2	0.523	12	0.426	48	**0.05**	0.69
ASTE1	0.325	12	0.473	47	**0.04**	0.67
BANP	0.483	12	0.570	43	0.23	1.00
C4orf6	0.434	10	0.253	47	**0.00**	0.07
CASP5	0.238	11	0.299	44	0.34	1.00
ELAVL3	0.191	10	0.246	45	0.31	1.00
GLYR1	0.177	11	0.268	50	0.30	1.00
LMAN1	0.179	11	0.201	50	0.98	1.00
MARCKS	0.341	11	0.414	42	0.28	1.00
NDUFC2	0.272	13	0.322	44	0.46	1.00
PTHLH	0.315	12	0.334	50	0.96	1.00
SLC22A9	0.409	12	0.379	44	0.70	1.00
SLC35F5	0.341	12	0.230	47	**0.05**	0.74
TAF1B	0.405	11	0.293	51	**0.01**	0.22
TCF7L2	0.381	8	0.318	43	0.41	1.00
TGFBR2	0.3944	11	0.466	44	0.50	1.00
ZNF294	0.469	12	0.486	53	0.79	1.00

(0%, 0/4 *B2M* mutation frequency) and 6 *MLH1*- or *MSH2* associated high stage (UICC III and IV) cancers (83.3%, 14/32 *B2M* mutation frequency) differed significantly ($p = 0.0476$).

4. Discussion

Carriers of a pathogenic *PMS2* variant represent a distinct group among Lynch syndrome patients, denoted mainly by a low penetrance, making *PMS2* a moderately penetrant gene at most (ten Broeke et al., 2015; Senter et al., 2008; Ten Broeke et al., 2018a; Goodenberger et al., 2016). However, recent work has suggested that tumors with PMS2 deficiency may demonstrate a more aggressive phenotype (Alpert et al., 2018). These observations suggest that there may be fundamental differences in the pathogenesis of PMS2-deficient CRCs that distinguish them from Lynch syndrome CRCs caused by germline variants affecting other MMR-genes such as *MLH1* and *MSH2*.

This study investigated the somatic cMS variant landscape of PMS2-deficient CRCs. In contrary to what we expected, we observed very similar somatic mutation patterns in PMS2-deficient CRCs versus MLH1- and MSH2-deficient CRCs. Of note, common mutational targets in MMR-deficient cancers such as *ACVR2* and *TGFBR2* were found to be mutant in all or the majority of analyzed PMS2-deficient CRCs. This implies that PMS2-deficient CRCs may develop through a pathogenetic mechanism with an impact of MMR-deficiency similar to other Lynch syndrome-associated cancers. Our results therefore support the hypothesis that MMR deficiency is a significant driving force of tumor development in the PMS2-deficient tumors analyzed, rather than representing merely an epiphenomenon.

In general, Lynch-associated CRCs appear to have better prognosis, which could be a consequence of increased immune activation due to cMS variant-induced frameshift neoantigens (Schwitalle et al., 2008; Kloor and von Knebel Doeberitz, 2016). However, a lower frequency of MSI-related features such as increased tumor-infiltrating lymphocytes (TILs) and Crohn-like infiltrate has previously been reported in PMS2-deficient tumors, suggesting a lower degree of immune activation (Alpert et al., 2018). This finding may also be causally related to the observation that CRCs with isolated PMS2 loss showed trends towards presenting with more distant metastasis and higher disease-specific death rates when compared to tumors due to pathogenic variants in other MMR genes. Similarly to Alpert et al., we also observed significantly lower CD3-positive T-cell infiltration in PMS2-deficient compared to other MMR-deficient CRCs. This difference remained significant even after adjusting for the UICC III/IV subgroup, which was more common in the PMS2 group.

Alpert et al. proposed an interesting hypothesis that a lower amount of mutational neoantigens may underlie the limited T-cell infiltration in

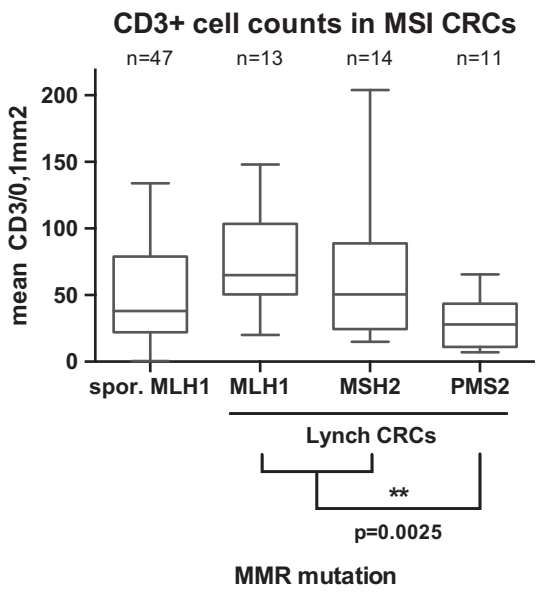

Fig. 2. Mean CD3-positive T-cell counts per 0.1 mm^2 are depicted as box plots for CRCs of *MLH1*, *MSH2* and *PMS2* variant carriers as well as a control group of sporadic MSI CRCs ("spor. MLH1"). Asterisks mark significantly lower median CD3-positive T-cell counts per 0.1 mm^2 in PMS2-deficient CRCs compared to those of *MLH1* and *MSH2* variant carriers.

these tumors. However, we could not confirm this hypothesis, as no significant differences between PMS2-deficient CRCs and MLH1- or MSH2-deficient CRCs were detected. As our data did not provide any evidence for a decreased amount of cMS mutation-induced frameshift peptides in PMS2-deficient CRCs on the DNA level, alternative explanations should be considered. It has recently been shown that loss of PMS2 appears to occur rather as a secondary event following neoplasia-inducing variant such as pathogenic *APC* variants. First, *KRAS* variants in PMS2-deficient CRCs, in contrast to those (G12D, G13D) typically observed in other Lynch syndrome-associated CRCs, rarely fit to the mutational signature of MMR deficiency (Alexandrov et al., 2013; Ahadova et al., 2018a; Ten Broeke et al., 2018b). Secondly, PMS2-deficient CRCs lack activating *CTNNB1* (β-catenin) variants, which are common in other Lynch syndrome-associated CRCs (Ahadova et al., 2018a; Ten Broeke et al., 2018b). Activating *CTNNB1* variants have been suggested to be associated with CRCs that develop from MMR-deficient crypts, i.e. CRCs initiated by MMR-deficiency (Ahadova et al., 2016; Ahadova et al., 2018b). Such tumors may develop more rapidly and potentially without an adenoma as precursor lesion that can be prevented by a polypectomy (Ahadova et al., 2016; Ahadova et al., 2018b). Indeed, prospective cohorts report a low or even absent CRC risk for *PMS2* carriers undergoing regular surveillance and polypectomies if needed (Moller et al., 2017; Moller et al., 2015). Third, normal PMS2 expression was detected in 16 adenomas from *PMS2* carriers, again underlining that PMS2 deficiency rather occurs as a secondary event (ten Broeke et al., 2019).

All these findings suggest that PMS2-deficient CRCs may resemble MMR-proficient CRCs in regards to tumor initiation and early evolution. Accordingly, immune evasion phenomena of PMS2-deficient CRCs may follow mechanisms recently described for MMR-proficient CRCs, for example local immune suppression related to Wnt signaling activation (Grasso and Giannakis, 2018). This hypothesis is further supported by our finding of only few *B2M* mutations among PMS2-deficient CRCs compared to MLH1- and MSH2-deficient CRCs. Immune evasion by inactivation of B2M is a well described event in MMR-deficient tumors (Kloor et al., 2010), which, however, occurs preferentially in an activated local immune environment, typically characterized by a high density of tumor-infiltrating lymphocytes (Echterdiek et al., 2016; Janikovits et al., 2018). Immunohistochemical characterization of immune cell infiltration suggest that this strong immunoselective pressure is lacking in PMS2-deficient CRCs.

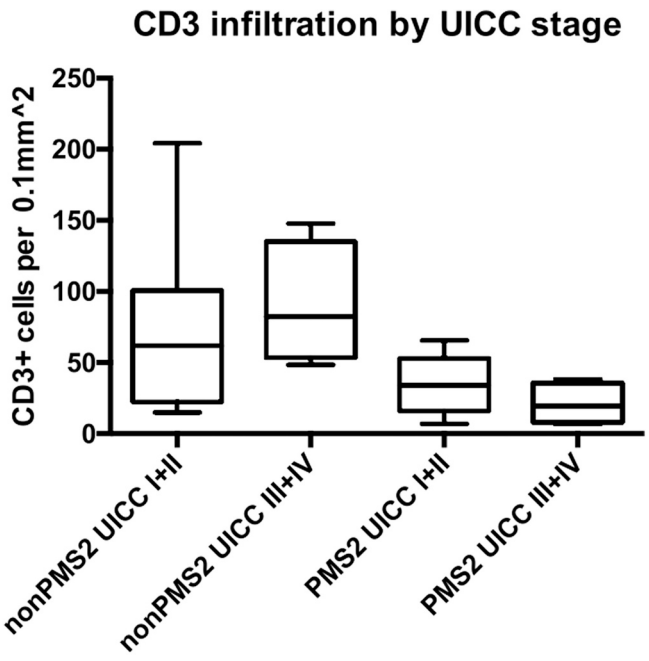

Table Analyzed	CD3stage
Column C	PMS2 UICC I+II
vs.	vs.
Column A	nonPMS2 UICC I+II
Mann Whitney test	
P value	0.2245
Exact or approximate P value?	Exact
P value summary	ns
Significantly different? (P < 0.05)	No
One- or two-tailed P value?	Two-tailed
Sum of ranks in column A,C	171 , 60
Mann-Whitney U	32
Difference between medians	
Median of column A	61.75, n=14
Median of column C	34.00, n=7
Difference: Actual	-27.75
Difference: Hodges-Lehmann	-24.28
95.39% CI of difference	-72.00 to 13.75
Exact or approximate CI?	Exact

Table Analyzed	CD3stage
Column D	PMS2 UICC III+IV
vs.	vs.
Column B	nonPMS2 UICC III+IV
Mann Whitney test	
P value	0.0286
Exact or approximate P value?	Exact
P value summary	*
Significantly different? (P < 0.05)	Yes
One- or two-tailed P value?	Two-tailed
Sum of ranks in column B,D	26 , 10
Mann-Whitney U	0
Difference between medians	
Median of column B	82.37, n=4
Median of column D	19.50, n=4
Difference: Actual	-62.87
Difference: Hodges-Lehmann	-59.87
97.14% CI of difference	-140.8 to -10.40
Exact or approximate CI?	Exact

Fig. 3. CD3-positive T-cell counts per 0.1 mm^2 are depicted as box plots for MSI CRCs of *MLH1* and *MSH2* variant carriers ("nonPMS2") and *PMS2* variant carriers, each divided into low stage (UICC I + II) and high stage (UICC III + IV) groups. CD3-positive T-cell count per 0.1 mm^2 after correction for tumor stage (UICC III + IV PMS2 vs. UICC III + IV MLH1/MSH2: 19.50 vs. 82.37, $p = 0.0286$).

Our results also imply that differences in cMS mutational spectrum do not directly explain the lower penetrance of pathogenic *PMS2* variants. One theory about the lower penetrance of *PMS2* variants is that the MLH3 or PMS1 proteins may take over part of the function of the PMS2 protein by forming a heterodimer with MLH1 in the absence of PMS2 (Peltomaki, 2003). Interestingly, the high prevalence of cMS variants in PMS2-deficient CRCs do not provide any evidence for a limited degree of MMR deficiency in these tumors after clinical manifestation. However, our study was limited by the number of analyzed tumor specimens and by focusing predominantly on cMS variants with putative driver function. For this reason, subtle or genome-wide differences may have been missed, as our panel was not designed to assess a general estimation of the quantitative level of MSI in PMS2-deficient tumors. Therefore, further studies on larger sample sets are required to validate our observation of a similar cMS spectrum for all MMR-gene variant carriers. Future studies will also be required to evaluate whether PMS2-deficient CRC patients with metastasized disease may benefit from immune checkpoint blockade using anti-PD-1 or anti-PD-L1 antibodies which

have shown very promising results in MMR-deficient cancer patients.

In conclusion, we observed surprisingly high amounts of somatic cMS variants in PMS2-deficient CRCs comparable to those observed in CRCs from *MLH1* and *MSH2* carriers. At the same time, we confirmed previous findings of limited T-cell infiltration in these tumors. Our data suggest that a low abundance of MMR-deficiency-induced mutational neoantigens does not seem to be an explanation for the limited local immune infiltration. Instead, we suggest that PMS2-deficient cancers, prior to inactivation of PMS2, may have acquired alternative mechanisms of immune cell exclusion typical of MMR-proficient CRCs. Larger studies including clinical follow-up data should explore the influence of the immune system on PMS2-deficient CRCs further. If confirmed, a lower immune response in *PMS2* carriers that develop CRC may have consequences for metastatic potential and overall prognosis.

Conflict of interest statement

The authors declare no potential conflicts of interest.

Ethics approval and consent to participate

The Institutional Ethics Committee, University Hospital Heidelberg (Protocol number: S-583/2016) approved the study. Informed consent was retrieved from all patients.

Funding

The study was performed with a financial support of the Dutch Cancer Society (UL 2012-5515) and the Wilhelm Sander Foundation (2016.056.1).

Author contributions

Study conception: S.W.B.t.B., A.B., A.A., M.v.K.D., M.N., M.K.

Molecular analysis: S.W.B.t.B., A.B., A.A., M.S., L.B., F.S., M.v.K.D., M.N., M.K.

Data analysis: S.W.B.t.B., A.B., A.A., M.S., L.B., F.S., J.K., A.B., N.F.d. M., M.v.K.D., M.N., M.K.

Data interpretation: S.W.B.t.B., A.B., A.A., M.S., L.B., F.S., H.M., T.v. W., N.F.d.M., M.v.K.D., M.N., M.K.

Manuscript writing: S.W.B.t.B., A.B., A.A., M.v.K.D., M.N., M.K.

Providing tissue specimens: M.v.K.D., M.N., M.K.

Revision and final approval of the manuscript: all authors.

Data availability statement

The datasets used and/or analyzed during the current study are available from the corresponding author on reasonable request.

Acknowledgments

The excellent support of Petra Höfler and Nina Nelius is highly appreciated.

Appendix A. Supplementary data

Supplementary data to this article can be found online at https://doi.org/10.1016/j.yexmp.2021.104668.

References

Ahadova, A., von Knebel, Doeberitz M., Bläker, H., Kloor, M., 2016. CTNNB1-mutant colorectal carcinomas with immediate invasive growth: a model of interval cancers in lynch syndrome. Familial Cancer 15 (4), 579–586.

Ahadova, A., Gallon, R., Gebert, J., Ballhausen, A., Endris, V., Kirchner, M., et al., 2018a. Three molecular pathways model colorectal carcinogenesis in lynch syndrome. Int. J. Cancer 143 (1), 139–150.

Ahadova, A., Gallon, R., Gebert, J., Ballhausen, A., Endris, V., Kirchner, M., et al., 2018b. Three molecular pathways model colorectal carcinogenesis in lynch syndrome. Int. J. Cancer.

Alexandrov, L.B., Nik-Zainal, S., Wedge, D.C., Aparicio, S.A., Behjati, S., Biankin, A.V., et al., 2013. Signatures of mutational processes in human cancer. Nature. 500 (7463), 415–421.

Alhopuro, P., Sammalkorpi, H., Niittymaki, I., Bistrom, M., Raitila, A., Saharinen, J., et al., 2012. Candidate driver genes in microsatellite-unstable colorectal cancer. Int. J. Cancer 130 (7), 1558–1566.

Alpert, L., Pai, R.K., Srivastava, A., McKinnon, W., Wilcox, R., Yantiss, R.K., et al., 2018. Colorectal carcinomas with isolated loss of PMS2 staining by immunohistochemistry. Arch. Pathol. Lab. Med.

Ballhausen, A., Przybilla, M.J., Jendrusch, M., Haupt, S., Pfaffendorf, E., Seidler, F., et al., 2020. The shared frameshift mutation landscape of microsatellite-unstable cancers suggests immunoediting during tumor evolution. Nat. Commun. 11 (1), 4740.

Barrow, E., Hill, J., Evans, D.G., 2013. Cancer risk in lynch syndrome. Familial Cancer 12 (2), 229–240.

Echterdiek, F., Janikovits, J., Staffa, L., Muller, M., Lahrmann, B., Fruhschutz, M., et al., 2016. Low density of FOXP3-positive T cells in normal colonic mucosa is related to the presence of beta2-microglobulin mutations in lynch syndrome-associated colorectal cancer. Oncoimmunology. 5 (2), e1075692.

Goodenberger, M.L., Thomas, B.C., Riegert-Johnson, D., Boland, C.R., Plon, S.E., Clendenning, M., et al., 2016. PMS2 monoallelic mutation carriers: the known unknown. Genet. Med. 18 (1), 13–19.

Grasso, C.S., Giannakis, M., 2018. Genomic mechanisms of immune evasion in colorectal cancer: from discovery to clinical practice. Oncotarget. 9 (73), 33743–33744.

Hause, R.J., Pritchard, C.C., Shendure, J., Salipante, S.J., 2016. Classification and characterization of microsatellite instability across 18 cancer types. Nat. Med. 22 (11), 1342–1350.

Janikovits, J., Muller, M., Krzykalla, J., Korner, S., Echterdiek, F., Lahrmann, B., et al., 2018. High numbers of PDCD1 (PD-1)-positive T cells and B2M mutations in microsatellite-unstable colorectal cancer. Oncoimmunology. 7 (2), e1390640.

Kim, T.M., Laird, P.W., Park, P.J., 2013. The landscape of microsatellite instability in colorectal and endometrial cancer genomes. Cell. 155 (4), 858–868.

Kloor, M., von Knebel Doeberitz, M., 2016. The immune biology of microsatellite-unstable cancer. Trends Cancer. 2 (3), 121–133.

Kloor, M., Michel, S., von Knebel Doeberitz, M., 2010. Immune evasion of microsatellite unstable colorectal cancers. Int. J. Cancer 127 (5), 1001–1010.

Le, D.T., Durham, J.N., Smith, K.N., Wang, H., Bartlett, B.R., Aulakh, L.K., et al., 2017. Mismatch-repair deficiency predicts response of solid tumors to PD-1 blockade. Science.

Moller, P., Seppala, T., Bernstein, I., Holinski-Feder, E., Sala, P., Evans, D.G., et al., 2015. Cancer incidence and survival in lynch syndrome patients receiving colonoscopic and gynaecological surveillance: first report from the prospective lynch syndrome database. Gut.

Moller, P., Seppala, T.T., Bernstein, I., Holinski-Feder, E., Sala, P., Gareth Evans, D., et al., 2017. Cancer risk and survival in path_MMR carriers by gene and gender up to 75 years of age: a report from the prospective lynch syndrome database. Gut.

Peltomaki, P., 2003. Role of DNA mismatch repair defects in the pathogenesis of human cancer. JClinOncol. 21 (6), 1174–1179.

Schwitalle, Y., Kloor, M., Eiermann, S., Linnebacher, M., Kienle, P., Knaebel, H.P., et al., 2008. Immune response against frameshift-induced neopeptides in HNPCC patients and healthy HNPCC mutation carriers. Gastroenterology. 134 (4), 988–997.

Senter, L., Clendenning, M., Sotamaa, K., Hampel, H., Green, J., Potter, J.D., et al., 2008. The clinical phenotype of lynch syndrome due to germ-line PMS2 mutations. Gastroenterology. 135 (2), 419–428.

ten Broeke, S.W., Brohet, R.M., Tops, C.M., van der Klift, H.M., Velthuizen, M.E., Bernstein, I., et al., 2015. Lynch syndrome caused by germline PMS2 mutations: delineating the cancer risk. J. Clin. Oncol. 33 (4), 319–325.

Ten Broeke, S.W., van der Klift, H.M., Tops, C.M.J., Aretz, S., Bernstein, I., Buchanan, D. D., et al., 2018a. Cancer risks for PMS2-associated lynch syndrome. J. Clin. Oncol. 36 (29), 2961–2968.

Ten Broeke, S.W., van Bavel, T.C., Jansen, A.M.L., Gomez-Garcia, E., Hes, F.J., van Hest, L.P., et al., 2018b. Molecular background of colorectal tumors from patients with lynch syndrome associated with germline variants in PMS2. Gastroenterology.

ten Broeke, S.W.S.M., Terlouw, D., Langers, A.M.J., Dekker, E., Tops, C.M.J., Vasen, H.F. A., van Wezel, T., Morreau, H., Nielsen, M., 2019. Incidence of Polyps and Incident Carcinomas in Patients with PMS2-Associated Lynch Syndrome: A Prospective Cohort Analysis.

Woerner, S.M., Benner, A., Sutter, C., Schiller, M., Yuan, Y.P., Keller, G., et al., 2003. Pathogenesis of DNA repair-deficient cancers: a statistical meta-analysis of putative real common target genes. Oncogene. 22 (15), 2226–2235.

Woerner, S.M., Yuan, Y.P., Benner, A., Korff, S., von Knebel, Doeberitz M., Bork, P., 2010. SelTarbase, a database of human mononucleotide-microsatellite mutations and their potential impact to tumorigenesis and immunology. Nucleic Acids Res. 38 (Database issue), D682–D689.